IJE TRANSACTIONS B: Applications Vol. 35, No. 05, (May 2022) 1024-1036

International Journal of Engineering

Journal Homepage: www.ije.ir

A Novel Curve for the Generation of the Non-circular Gear Tooth Profile

N. H. Thai*[a], N. T. Trung[b]

[a] Hanoi University of Science and Technology, Hanoi, Vietnam
[b] National Research Institute of Mechanical Engineering, Hanoi, Vietnam

PAPER INFO

Paper history:
Received 26 January 2022
Received in revised form 20 Febraury 2022
Accepted 21 Febraury 2022

Keywords:
Non-circular Gear
Rack Cutter
Undercutting
Novel Curve
Line of Meshing

ABSTRACT

This paper presents a novel curve generated by a point attached to an ellipse as it rolls without slipping along a datum line of rack cutter. A mathematical model of the non-circular gear profile has been developed based on the theory of gearing. The effect of an axial ratio λ (the ratio of the lengths of the major and minor axes of the ellipse) and the position of the point K_R, at which the novel curve starts to generate on the tooth shape and the undercut of the non-circular gear pair is also taken into consideration. A numerical program developed from the mathematical model has been proposed for the calculation and design of the non-circular gears (NCGs). Case studies are presented to show the steps of tooth shape design and to examine the geometrical profile of the NCGs in relation to design parameters of the rack cutter etc. From that, the axial ration λ and position of the point K_R on the generating ellipse Σ_E can be selected for each specific case in order to design the appropriate profiles of the NCGs. On that basis, an experiment to determine the gear ratio of the NCGs pair based on the meshing between gears has manufactured.

***doi**: 10.5829/ije.2022.35.05.18*

1. INTRODUCTION

Non-circular gears (NCGs) is designed to generate continuously variable transmission with high accuracy. Due to complexity in design and fabrication difficulties, the application of NCGs in practice still has many limitations [1]. In spite of the fact that NCGs are not commonly used as circular gear, the NCGs have been applied in various machines and equipment such as agricultural machinery [2-4]; medical equipment [5]; coal seam gas drainage machine [6]; hydraulic motors [7]; steering robotic mechanisms (with elliptical gears) [8] etc. Therefore, the NCGs have drawn a lot of interest from scientists with the following trends: (1) Generation of centrodes based on a transfer function of mechanisms [4, 5, 9]; (2) Design of the NCGs tooth profile by a number of methods such as: (a) Using shaper cutter [10, 11]; (b) Using rack cutter with an isosceles trapezoidal profile or circular arc profile [12-14]; (3) Design non-circular gearing systems for various applications [15-17]. Recently, Hao et al. [18] proposed methods to design an NCGs pair based on an arbitrary centrode. However, those NCGs pairs could only be used for low-load application because the effect of undercutting and interference was not taken into the design process; (4) Methods for manufacturing the NCGs spur and the NCGs helical were the research object of other researchers [19-21]. Among those four trends, NCGs tooth profile design has drawn the most interest. The majority of the research focused on using circle involute [10, 12, 22]; or circular arc [13, 23] to generate the NCGs tooth profile. A setback in these works is the difference in shape and dimension of the teeth located around NCGs since these are gears with asymmetrical tooth profiles. The NCGs is different from standard cylindrical gears with the constant gear ratio [24-26]. The tooth thickness changes along with centrodes in the generation by a standard rack-cutter, and at places where the radius of the centrodes is small, the tooth are often undercutting. Thus, it is necessary to reduce the pressure angle of the cutter, but it causes undercutting or interference. In addition, when using traditional tooth profiles such as circle involute and a

*Corresponding Author Email: thai.nguyenhongr@hust.edu.vn (N. H. Thai)

Please cite this article as: N. H. Thai, N. T. Trung, A Novel Curve for the Generation of the Non-circular Gear Tooth Profile, ***International Journal of Engineering, Transactions B: Applications***, Vol. 35, No. 05, (2022) 1024-1036

circular arc to design the tooth profile of the NCG to satisfy the condition of undercutting, the number of teeth distributed on gear must be significant. That results in often small tooth sizes reducing the gear drive load capacity.

In this study, to overcome the above problems, we proposed a novel curve in the tooth profile design of the NCGs. This primarily ensures that the teeth in different positions on the gear are more evenly distributed and the tooth size is larger to increase the load capacity of the gear drive. Compared to the other research, this paper focuses on building a mathematical model for the new curve and determining the conditions for applying it to the design of the tooth profile of the NCGs.

This paper is organized as follows: The mathematical model of the novel curve is presented in section 2. Section 3 presents the novel curve's application to the rack cutter's design. The method of applying the novel profile to the tooth design of the NCGs is presented in section 4. Conditions to avoid undercutting are presented in section 5. Meanwhile, illustrative examples verifying the applicability of the novel profile in the NCGs designs are presented in section 6. Section 7 presents the manufacturing of an NCG drive and experimental measurements to verify the applicability of the novel profile in practice. Finally, the results of the study are presented in section 8.

2. ESTABLISHMENT OF MATHEMATICAL MODEL OF THE NOVEL CURVE

The novel curve Γ_R is generated by an arbitrary point K_R attached to an ellipse Σ_E, with Σ_E rolls without sliding above or below a line Δ as described in Figure 1a.

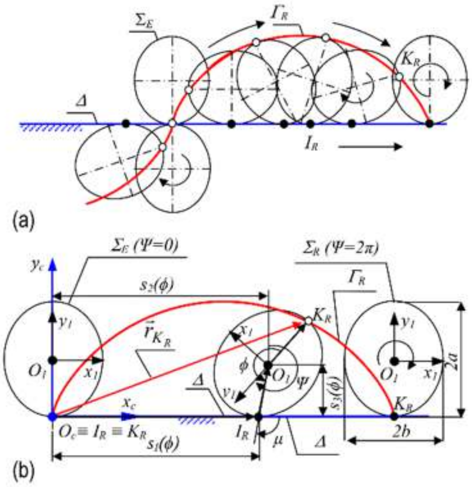

Figure 1. Movement of the generating ellipse with a) The novel curve and b) Principle of elliptical path traced

To establish the mathematical model of the novel curve Γ_R, from Figure 1b, we have: $\vartheta_c\{O_c x_c y_c\}$ is the fixed coordinate systems rigidly attached on the line Δ; $\vartheta_1\{O_1 x_1 y_1\}$ is a coordinate system attached to the center O_1 of the generating ellipse Σ_E; the point I_R is a mating point between the ellipse Σ_E and the line Δ when Σ_E rolls without sliding on Δ. There are two movements of the generating ellipse Σ_E: (1) The center O_1 of Σ_E translates in the direction x_c by the distance $s_2(\psi)$ and translates in the direction y_c by the distance $s_3(\psi)$, where ψ is the rotation angle of the coordinate system $\vartheta_1\{O_1 x_1 y_1\}$ in relation with the coordinate system $\vartheta_c\{O_c x_c y_c\}$; (2) Σ_E rotates around O_1 an angle ψ. In the coordinate system $\vartheta_c\{O_c x_c y_c\}$ attached to Δ as described in Figure 1a, beginning moment Σ_E contacts Δ at the point $O_c \equiv I_R \equiv K_R$. After an interval of time, when the point I_R have translated a distance $\overline{O_c I_R}$ from O_c to I_R in Δ, the ellipse Σ_E will move by an arch $\widehat{e}$ from I_R to K_R on Σ_E and make a rotation angle ψ. Therefore, we have:

The relative position of the mating point I_R with respect to O_c is determined by:

$$s_1(\phi) = \widehat{e} = \int_0^{\phi} \sqrt{r_E(\phi)^2 + \left(\frac{dr_E(\phi)}{d\phi}\right)^2}\, d\phi \tag{1}$$

wherein: $r_E(\phi)$ is the polar radius of Σ_E. From literature [23], $r_E(\phi)$ is given by:

$r_E(\phi) = a\sqrt{\dfrac{1-\varepsilon^2}{1-\varepsilon^2\cos^2\phi}}$ with $\varepsilon = \dfrac{\sqrt{a^2-b^2}}{a}$ and a, b are the major axis and minor axis of Σ_E, respectively; $\phi = \angle(O_1K_R, O_1I_R)$ is the angle of the arch $\widehat{e}$ on Σ_E.

(i) The relative position of O_1 with respect to O_c when Σ_E rolls without sliding on Δ is given by:

In direction of x_c:

$$s_2(\phi) = s_1(\phi) + r_{I_R}(\phi)\sin(\psi - \phi) \tag{2}$$

In direction of y_c:

$$s_3(\phi) = r_{I_R}(\phi)\cos(\psi - \phi) \tag{3}$$

(ii) The generating ellipse Σ_E rotates around O_1 an angle ψ:

$$\phi = \psi + \mu - \frac{\pi}{2} \tag{4}$$

where: $\mu = \arctan\left(\dfrac{\partial x_E(\phi)/\partial\phi}{\partial y_E(\phi)/\partial\phi}\right)$

By transformation coordinates of K_R from $\vartheta_1\{O_1 x_1 y_1\}$ system to $\vartheta_c\{O_c x_c y_c\}$, equation of the novel curve is obtained by:

$$\mathbf{r}_{K_R} = {}^{c}\mathbf{r}_{I_R} + {}^{c}\mathbf{r}_{O_1} + {}^{c}\mathbf{M}_1 {}^{1}\mathbf{r}_{K_R} \tag{5}$$

wherein: ${}^{1}\mathbf{r}_{K_R} = [0 \ \ -a \ \ 0]^T$;

${}^{c}\mathbf{r}_{O_1} = [s_2(\psi) \ \ s_3(\psi) \ \ 0]^T$; ${}^{c}\mathbf{r}_{I_R} = [s_1(\phi) \ \ 0 \ \ 0]^T$;

$${}^{c}\mathbf{M}_1 = \begin{bmatrix} \cos\psi(\phi) & \sin\psi(\phi) & 0 \\ -\sin\psi(\phi) & \cos\psi(\phi) & 0 \\ 0 & 0 & 1 \end{bmatrix}$$

After transforming, Equation (5) is rewritten as:

$$\mathbf{r}_{K_R} = \begin{bmatrix} x_{K_R} \\ y_{K_R} \\ 0 \end{bmatrix} = \begin{bmatrix} s_2(\phi) - a\sin(\psi) \\ (-1)^g s_3(\phi) - a\cos(\psi) \\ 0 \end{bmatrix} \tag{6}$$

In Equation (6): $g = 0$ when Γ_R is about Δ and $g = 1$ when Γ_R is below Δ.

3. PROFILE GENERATION OF THE RACK CUTTER BY THE NOVEL CURVE

3. 1. Determination of Design Parameters of the Rack Cutter by the Novel Curve

From the novel curve mathematical model set up in section 1, the formation of the rack cutter profile is shown in Figure 2.

In this figure (Figure 2, above) the datum line of the rack cutter Δ is the dedendum profile and below Δ is the addendum profile. The design parameters are determined as follows:

The pitch p_c

According to the method for the novel curve generation, both of the tooth thickness t and the space width w on the pitch line of the rack cutter will be equal to the perimeter of the generating ellipse Σ_E:

$$t = w = C_{\Sigma_{RE}} \tag{7}$$

wherein: $C_{\Sigma_E} = \int_0^{2\pi} \sqrt{r_E(\phi)^2 + \left(\frac{dr_E(\phi)}{d\phi}\right)^2}\, d\phi$

Therefore, the pitch on the centrode of the rack cutter can be calculated as follows:

$$p_c = t + w = 2C_{\Sigma_{RE}} \tag{8}$$

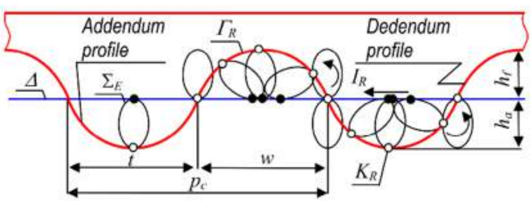

Figure 2. New rack cutter

The tooth height h

The addendum height h_a and dedendum height h_f when the point K_R is located at the major and minor axis of Σ_E are represented in the following equations:

$$\begin{cases} h_a = h_f = 2(pa + qb) \\ h = h_a + h_b = 4(pa + qb) \end{cases} \tag{9}$$

wherein: $p = 1$, $q = 0$ when the point K_R is attached to the major axis of Σ_E and $p = 0$, $q = 1$ when the point K_R is attached to the minor axis of Σ_E.

3. 2. Influence of the Elliptical Parameters and the Starting Point Position on the Tooth Profile of the Rack Cutter

From sections 1.1 and 1.2, it is noticeable that the profile of the rack cutter is dependent on: (1) the position of the point K_R attached to Σ_E; (2) the ratio $\lambda = a/b$ of the generating ellipse Σ_E. Let further consider the following two cases:

Case 1: *Influence of the position of K_R on the tooth profile of the rack cutter*

We have $\beta = \angle(O_1y_1, O_1I_0)$ is the angle defining the position of the point K_R attached to Σ_E (see Figure 3). Because of symmetry about the semi axes, only the position of K_R in the fourth quarter of Σ_E is taken into consideration. Influence of the position of K_R fixed on Σ_E on the tooth profile of the rack cutter is investigated with $\beta \in [0 \div \pi/2]$, increments $\Delta\beta = \pi/8$, and the pitch of centrode of the rack cutter p_c = *19.6* mm. The design parameters of the rack cutter are given in Table 1 and Figure 3 shows the corresponding profile of the rack cutter.

From Figure 3 and Table 1 we have: (i) When the point K_R fixed on Σ_E is located on the major axis or minor axis ($\beta = 0$° and $\beta = 90$°), the profile of the rack cutter will be symmetrical and the tooth heights will be as follows $h|_{\beta=0^o} > h|_{\beta=90^o}$; (ii) When $0^o < \beta < 90^o$, the tooth height will increase in the range $4b < h < 4a$, and the tooth profile will be asymmetrical and deviated to the left.

***Case 2:** Influence of the ratio $\lambda = a/b$ of the generating ellipse on the tooth profile of the rack cutter*

TABLE 1. Design parameter of the rack cutter by the position of K_R attached to Σ_E

β (°)	a (mm)	b (mm)	p_c (mm)	h (mm)
0.0	1.75	1.36	19.6	7.0
22.5	1.75	1.36	19.6	6.8
45.0	1.75	1.36	19.6	6.4
90.0	1.75	1.36	19.6	5.4

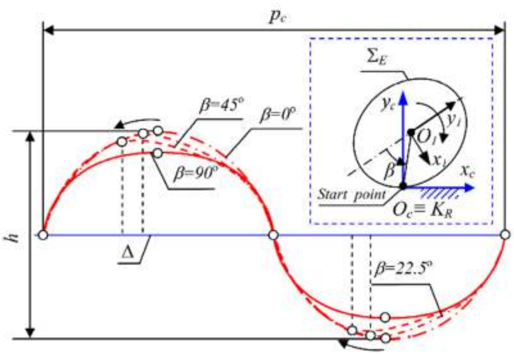

Figure 3. Profile of the rack cutter corresponding to different starting points K_R

In this case, the ratio λ is obtained from Equation (7). With p_c is kept to be equal to *19.6 mm*, the ration λ will have the values of 1.29, 1.00, 0.78, 0.52, respectively. When the point K_R is on the semi-major axis vertex, the design parameters of the rack cutter corresponding to λ will be shown in Table 2. The profile or the rack cutter is presented in Figure 4.

From Figure 4 and Table 2 we have:

(i) The tooth height h decreases with smaller values of λ; (ii) When λ decreases, the tooth addendum turns into a concave form. It can be explained as while λ decreases, the major semi axis becomes semi-minor axis, at the position K_R^* of Σ_E after rolling on Δ, distance

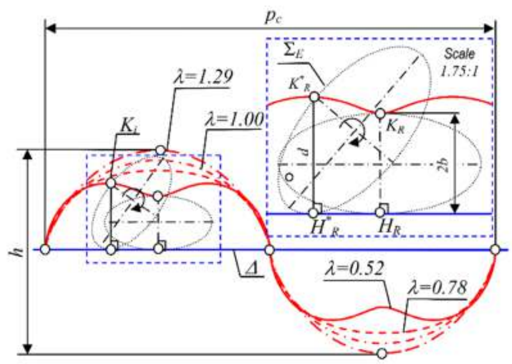

Figure 4. The tooth profiles corresponding to different values of λ

TABLE 2. Design parameters of the rack cutter corresponding to λ of Σ_E

λ	*a* (mm)	*b* (mm)	p_c (mm)	*h* (mm)
1.29	1.75	1.36	19.6	7.0
1.00	1.56	1.56	19.6	6.2
0.78	1.36	1.75	19.6	5.4
0.52	1.05	2.00	19.6	4.7

$d = \overline{H_R^* K_R^*} > 2b$ will cause concavity on the addendum (inside the area covered by the dashed line in Figure 4). This phenomenon will be resolved in the following section 2.3; (iii) When λ = 1, the ellipse Σ_E becomes circle, and the profile Γ_R of the rack cutter changes into cycloidal curve.

3. 3. Condition for Convexity of the Rack Cutter Profile

From Figure 4 *(area bordered by the dashed line)* with $\lambda = 0.52$ *(point K_R lies on the semi-minor axis vertex of Σ_E)*, the profile will be concave. To achieve the convexity of the curve Γ_R, it is necessary to determine the relationship between parameters *a* and *b* of Σ_E. Therefore, if we consider the ellipse is fixed, the tangency Δ only rolls on the ellipse, and I_R is the contact point between them (Figure 5); the problem will be transformed into finding distances from the point K_R on the minor semi-axis vertex to tangents Δ of the ellipse.

The tangent Δ to the ellipse at the point I_R can be expressed by the following equation:

$$\frac{x_{I_R}(\phi)x}{b^2} + \frac{y_{I_R}(\phi)y}{a^2} = 1 \tag{10}$$

where: $x_{I_R}(\phi) = b\cos\phi, y_{I_R}(\phi) = a\sin\phi$

Equation (10) can be rewritten thus:

$$\cos\phi ax + \sin\phi by - ab = 0 \tag{11}$$

Distance from the point K_R *(b, 0)* to the tangent Δ of Σ_E at I_R is described as follows:

$$f(\phi) = d(K_\Gamma, \Delta) = \frac{|ab\cos\phi - ab|}{\sqrt{(a\cos\phi)^2 + (b\sin\phi)^2}} \tag{12}$$

By solving equation $\frac{df(\phi)}{d\phi} = 0$; finding the extremes of $f(\phi)$ at $\sin\phi = 0$ and $\cos\phi = \frac{-a^2}{a^2+b^2}$; and substituting into Equation (12), the maximum value of *d* is given by:

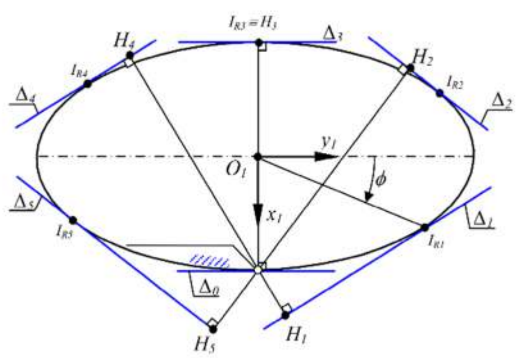

Figure 5. Distances from the point K_Γ to tangents Δ

$$d_{\max} = \frac{ab(a + a^2 + b^2)}{\sqrt{(b^4 a^2 + 3b^2 a^4 - a^4 + a^6)}} \tag{13}$$

From Figure 4, the profile becomes concave when $d < 2b$. Together with Equation (13), the condition of convexity of Γ_R can be inequality as below:

$$b \geq \frac{ab(a + a^2 + b^2)}{2\sqrt{(b^4 a^2 + 3b^2 a^4 - a^4 + a^6)}} \tag{14}$$

4. MATHEMATICAL MODEL OF THE ELLIPSE NON-CIRCULAR GEAR SURFACES

4. 1. Equation of the Centrode of the NCGs Pair

There are two usual approaches for designing the centrodes: (1) To establish the conjugated centrodes Σ_i *(i =1, 2)* when the gear ratio function $i_{12}(\phi_1)$ is given in advance; (2) To determine the conjugated centrodes Σ_i when one centrode and the center distance of the gear pair are given. In this work, the second approach was utilized. The center distance A_{12} and one centrode, which is an eccentric circle $\Sigma_1(O_1, R)$, are given. From Figure 6 if $r_1(\phi_1)$ is a polar radius of the centrode $\Sigma_1(O_1,R)$ corresponding to an angular polar ϕ_1; $r_2(\phi_2)$ is a polar radius of the centrode $\Sigma_2(O_2,r_2(\phi_2))$ corresponding to an angular polar $\phi_2(\phi_1)$; and the point I is the instantaneous center. According to Mundo [15], the equations of the centrodes of the NCGs is described as follows:

$$\begin{cases} r_2(\phi_2) = r_2(\phi_2(\phi_1)) = A_{12} - r_1(\phi_1) \\ \phi_2(\phi_1) = \int_0^{\phi_1} i_{21} d\phi_1 \end{cases} \tag{15}$$

where: $i_{21}(\phi_1) = \dfrac{r_1(\phi_1)}{A_{12} - r_1(\phi_1)}$ is the gear ratio function of the NCGs pair; stated in the literature [27] $r_1(\phi_1) = \sqrt{(R^2 - e^2 \sin^2 \phi_1)} - e\cos\phi_1$ with R is a radius of a circle $\Sigma_1(O_1,R)$ and e is an eccentricity of the rotation center O_1 from the center of the circle $\Sigma_1(O_1,R)$ as shown in Figure 6.

The relationship between the revolutions of the driving gear and the driven gear is given by the following equation [24]:

$$2\pi = n_2 \int_0^{2\pi} \left(\frac{r_1(\phi_1)}{A_{12} - r_1(\phi_1)} \right) d\phi_1 \tag{16}$$

where n_2 is the number of revolutions that centrode Σ_1 performs for one revolution of centrode Σ_2.

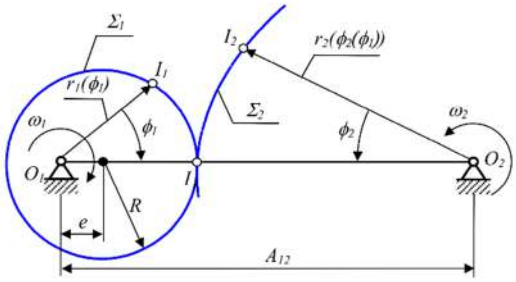

Figure 6. Illustration of mating centrodes 2 versus 1

4. 2. A Mathematical Model of the Profile of the NCGs Pair Generated by the Novel Rack Cutter

In general, the relative motion between the novel rack cutter and the NCGs in the fixed coordinate system $\vartheta_f\{O_f x_f y_f\}$ is described in Figure 7. Where $\vartheta_c\{O_c x_c y_c\}$ is a coordinate system connected to the datum line Δ of the rack Σ_R; $\vartheta_i\{O_i x_i y_i\}$ is a coordinate system connected to the gear; the point I is the instantaneous center and also is the mating point between Δ and the centrode curve Σ_i of the gear *(i = 1, 2 when generating a profile of the driving and driven gear, respectively*); $\psi_i = \phi_i + \mu_i - \dfrac{\pi}{2}$ is an angular position of the coordinate system $\vartheta_i\{O_i x_i y_i\}$ in reference to the coordinate system $\vartheta_f\{O_f x_f y_f\}$ during generating

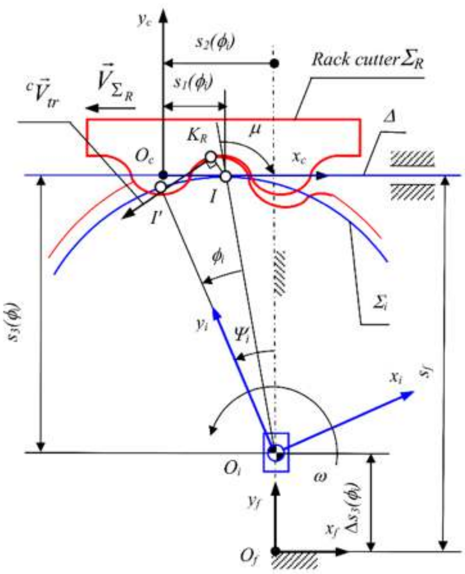

Figure 7. Relative motion between the rack cutter and the NCGs

process with $\mu_i = \arctan\left(\dfrac{r_i(\phi_i)}{dr_i/d\phi_i}\right)$; s_f is a distance from x_c to x_f; $s_1(\phi_i) = \int_0^{\phi_i} \sqrt{r_i(\phi_i)^2 + \left(\dfrac{dr_i(\phi_i)}{d\phi_i}\right)^2}\, d\phi_i$ is a displacement of the rack cutter along direction x_f, $s_3(\phi_i) = r(\phi_i)\cos(\psi_i - \phi_i)$ is a displacement of the NCGs center O_i along direction y_f when the point I of Σ_i moves to the position I'.

Based on the equation of the NCGs centrode in section 3.1, the profile of the NCGs will be generated by the rack cutter Σ_R. According to literature [1, 13, 14] and from Figure 7, the relative motion between the NCGs and the rack cutter Σ_R contains the following movements:

(1) The rack cutter translates a distance $s_2(\phi_i) = s_1(\phi_i) + r_i(\phi_i)\sin(\psi - \phi_i)$ along the direction of x_f;

(2) The gear sequentially moves as follows: (a) The geared center O_i translates a distance $\Delta s_3(\phi_i) = s_{fi} - s_3(\phi_i)$ along the direction of y_f; (b) The gear rotates around O_i an angle ψ_i.

Therefore, if K_R is the shaping point on Γ_R of Σ_R, and by transforming the coordinates of K_R from $\vartheta_c\{O_c x_c y_c\}$ to $\vartheta_i\{O_i x_i y_i\}$ of the gear, the profile equation of the shaped gear is expressed by:

$$\mathbf{r}_{K_i} = {}^i\mathbf{M}_f \mathbf{M}_f {}^f\mathbf{M}_c\, \mathbf{r}_{K_R} \tag{17}$$

wherein:

$${}^f\mathbf{M}_c = \begin{bmatrix} 1 & 0 & s_2(\phi_i) \\ 0 & 1 & s_{fi} \\ 0 & 0 & 1 \end{bmatrix}; \quad \mathbf{M}_f = \begin{bmatrix} 1 & 0 & 0 \\ 0 & 1 & \Delta s_3(\phi_i) \\ 0 & 0 & 1 \end{bmatrix};$$

$${}^i\mathbf{M}_f = \begin{bmatrix} \cos\psi_i & \sin\psi_i & 0 \\ -\sin\psi_i & \cos\psi_i & 0 \\ 0 & 0 & 1 \end{bmatrix};$$

$\mathbf{r}_{K_R}$ is determined from Equation (6). The relationship between the kinematic parameter ϕ_i and the geometrical parameter ϕ is expressed by the meshing equation [27]:

$$\mathbf{n}\,{}^c\mathbf{V}_{tr} = 0 \tag{18}$$

where: $\mathbf{n}^c$ is the common normal vector of the conjugated profiles (Γ_i, Γ_R) at the mating point K. ${}^c\mathbf{V}_{tr}$ is the relative sliding velocity between $K_R \in \Gamma_R$ and $K_i \in \Gamma_i$ at K, when Γ_i are rolling as well as slipping with Γ_R. The vector $\mathbf{n}$ is given by:

$$\mathbf{n} = \frac{\partial \mathbf{r}_{K_R}(\phi)}{\partial \phi} \times \mathbf{k} \tag{19}$$

With $\mathbf{k} = [0 \quad 0 \quad 1]^T$, and ${}^c\mathbf{V}_{tr}$ is expressed as below:

$${}^c\mathbf{V}_{tr} = \omega_c \times {}^c\mathbf{r}_{IK} \tag{20}$$

where: $\omega_c = \omega_c \mathbf{k}_c$ is the angular velocity of the shaped gear in relation with the coordinate system $\vartheta_c\{O_c x_c y_c\}$ of the rack cutter, and ${}^c\mathbf{r}_{IK} = (s_1(\phi) - x_{K_R})\mathbf{i}_c + y_{K_R}\mathbf{j}_c$

By transforming ${}^c\mathbf{V}_{tr}$, one gets:

$${}^c\mathbf{V}_{tr} = \omega \begin{bmatrix} -y_{K_R} \\ s_1(\phi) - x_{K_R} \end{bmatrix} \tag{21}$$

Substituting Equations (19) and (21) into Equation (18), it is possible to write:

$$f(\phi, \phi_i) = y'_{K_R}(\phi) y_{K_R}(\phi) + x'_{K_R}(\phi)(s_1(\phi_i) - x_{K_R}(\phi)) = 0 \tag{22}$$

By solving Equation (22), the relationship between ϕ_i and ϕ of the gear i with the rack cutter.

4. 2. 1. The Profile Equation of the Driving Gear

Because the driving gear is the eccentric circle gear, the parameters of the shaping movements are given by:

$$s_1(\phi_1) = \int_0^{\phi_i} \sqrt{r_1(\phi_1)^2 + \left(\frac{dr_1(\phi_1)}{d\phi_1}\right)^2}\, d\phi_i \tag{23}$$

$$s_2(\phi_1) = s_1(\phi_1) + r_1(\phi_1)\sin(\psi_1 - \phi_1) \tag{24}$$

$$s_3(\phi_1) = r_1(\phi_1)\cos(\psi_1 - \phi_1) \tag{25}$$

$$\Delta s_3(\phi_1) = s_{f1} - s_3(\phi_1) \tag{26}$$

wherein: $s_{f1} = R + e$, and by substituting equations from Equation (23) to Equation (26) into Equation (17), the profile equation of the driving eccentric circular gear is expressed as follows:

$$\mathbf{r}_{K1} = \begin{bmatrix} (s_3(\phi_1) + y_{K_R})\cos\psi_1 + (s_2(\phi_1) - x_{K_R})\sin\psi_1 \\ (s_3(\phi_1) + y_{K_R})\sin\psi_1 - (s_2(\phi_1) - x_{K_R})\cos\psi_1 \\ 0 \end{bmatrix} \tag{27}$$

4. 2. 2. The Profile Equation of the Driven Gear

The non-circular driven gear has a polar radius $r_2(\phi_2(\phi_1)) = A_{12} - r_1(\phi_1)$ determined by Equation (15). The parameters of the shaping movements of this driven gear are given by the following equations:

$$s_1(\phi_2(\phi_1)) = \int_0^{\phi_2} \sqrt{r_1(\phi_2(\phi_1))^2 + \left(\frac{dr_1(\phi_2(\phi_1))}{d\phi_2(\phi_1)}\right)^2}\, d\phi_2(\phi_1) \tag{28}$$

$$s_2(\phi_2(\phi_1)) = s_1(\phi_2(\phi_1)) + r_2(\phi_2(\phi_1))\sin(\psi_2 - \phi_2(\phi_1)) \quad (29)$$

$$s_3(\phi_2(\phi_1)) = r_2(\phi_2(\phi_1))\cos(\psi_2 - \phi_2(\phi_1)) \quad (30)$$

$$\Delta s_3(\phi_2(\phi_1)) = s_{f2} - s_3(\phi_2(\phi_1)) \quad (31)$$

where $s_{f1} = A_{12} - R + e$, and by substituting equations from Equation (28) to Equation (31) into Equation (17), the equation of the NCGs profile is obtained as follows:

$$\mathbf{r}_{K_2} = \begin{bmatrix} (s_3(\phi_2(\phi_1)) + y_{K_R})\cos\psi_2 + (s_2(\phi_2(\phi_1)) - x_{K_R})\sin\psi_2 \\ (s_3(\phi_2(\phi_1)) + y_{K_R})\sin\psi_2 - (s_2(\phi_2(\phi_1)) - x_{K_R})\cos\psi_2 \\ 0 \end{bmatrix} \quad (32)$$

5. TOOTH UNDERCUTTING AND THE LINE OF MESHING

5. 1. Tooth Undercutting From literature [28, 29], to avoid undercutting during the profile shaping process, the equation of the tooth profile needs to satisfy:

$$\Delta_1^2 + \Delta_2^2 = 0 \quad (33)$$

wherein:

$$\Delta_1 = \begin{vmatrix} \dfrac{dx_{K_R}}{d\phi} & -{}^cV_{trx} \\ \dfrac{\partial f(\phi)}{\partial \phi} & \dfrac{\partial f(\phi_i)}{\partial \phi_i}\dfrac{d\phi_i}{dt} \end{vmatrix}; \Delta_2 = \begin{vmatrix} \dfrac{dy_{K_R}}{d\phi} & -{}^cV_{try} \\ \dfrac{\partial f(\phi)}{\partial \phi} & \dfrac{\partial f(\phi_i)}{\partial \phi_i}\dfrac{d\phi_i}{dt} \end{vmatrix}$$

With ${}^cV_{trx}$, ${}^cV_{try}$ are the components of the sliding velocity of the shaping point K_R on the profile of the rack cutter Γ_R. By further developing of Δ_1, Δ_2 one obtains:

$$\begin{cases} \Delta_1 = A_1 - B_1 C_1 \\ \Delta_2 = A_2 - B_2 C_2 \end{cases} \quad (34)$$

wherein:

$A_1 = \rho_i(C_1 - EH - GFI + J);\ B_1 = -NGF$

$A_2 = \rho_i(-EF - GHI + J(1+I));\ B_2 = M - s_1(\phi)$

$C_1 = C_2 = (G^2 + E^2)^{0.5};\ E = \dfrac{a\varepsilon^2 \sin 2\phi(\varepsilon^2 - 1)^{0.5}}{2(\varepsilon^2\cos^2\phi - 1)^{1/5}}$

$F = \dfrac{\cos\phi(1-\varepsilon^2)}{(1 - 2\varepsilon^2\cos^2\phi + \varepsilon^4\cos^4\phi)^{0.5}};\ G = a\left(\dfrac{1-\varepsilon^2}{1-\varepsilon^2\cos^2\phi}\right)^{0.5}$

$H = \dfrac{\sin\phi}{(1-2\varepsilon^2\cos^2\phi + \varepsilon^4\cos^4\phi)^{0.5}};\ I = \dfrac{a^2b^2}{a^4 - (a^4 - b^4)\cos^2\phi}$

$J = \dfrac{a\varepsilon^2}{(1-2\varepsilon^2\cos^2\phi + \varepsilon^4\cos^4\phi)^{0.5}}$

$M = a\dfrac{(1-\varepsilon^2)^{0.5} - \varepsilon^2\cos\phi\sin\phi(1-\varepsilon^2\cos^2\phi)}{((1-\varepsilon^2\cos^2\phi)(1-2\varepsilon^2\cos^2\phi + \varepsilon^4\cos^4\phi))^{0.5}}$

$N = a\left(\dfrac{\sin^2\phi - \cos^2\phi(1-\varepsilon^2)}{(1-2\varepsilon^2\cos^2\phi + \varepsilon^4\cos^4\phi)^{0.5}}\right)$

5. 1. 1. For the Driving Gear Because $\Sigma_1(O_1, R)$ is the eccentric circle, the curvature radius at each point on Σ_1 is constant and equal to R:

$$\rho_1(\phi_1) = R \quad (35)$$

5. 1. 2. For the Driven Gear From literature [1, 23], the curvature radius $\rho_2(\phi_2)$ of Σ_2 is determined as follows:

$$\rho_2(\phi_2) = \frac{\sqrt{\left(r_2(\phi_2)^2 + \left(\dfrac{dr_2(\phi_2))}{d\phi_2}\right)^2\right)^3}}{r_2(\phi_2)^2 + 2\left(\dfrac{dr_2(\phi_2)}{d\phi_2}\right)^2 - r_2(\phi_2)\dfrac{d^2r_2(\phi_2)}{d\phi_2{}^2}} \quad (36)$$

wherein: $r_2(\phi_2)$ is obtained from Equation (15).

5. 2. The Line of Meshing The curve ζ_K is a locus of the contact point K of the conjugated profiles (Γ_1, Γ_2), with Γ_1 belongs to the driving gear, and Γ_2 is the driven one, as shown in Figure 8. This curve ζ_K can also be called the line of meshing, with the point K is the mating point. At the mating moment $K \equiv K_1 \equiv K_2$, with $K_1 \in \Gamma_1$, $K_2 \in \Gamma_2$. On the same time when $K_1 \in \Gamma_1$ there is a corresponding point $I_1 \in \Sigma_1$, and similarly, with $K_2 \in \Gamma_2$ there is $I_2 \in \Sigma_2$ ($I_1 \equiv I_2 \equiv I$). Therefore, when the driving gear rotates around O_1 an angle $\phi_1 = \angle(O_1I_1, O_1I)$ to place I_1 on Σ_1 to the position of the pitch point I on O_1O_2 ,the driven gear correspondingly rotates around O_2 an angle $\phi_2(\phi_1) = i_{21}(\phi_1)\phi_1 = \angle(O_2I_2, O_2I)$ to move I_2 on Σ_2 to the pitch point I following gear ratio function $i_{12}(\phi_1)$.

The equation of the line of meshing ζ_K can be expressed as follows:

$$\mathbf{r}_{\zeta_K} = {}^f\mathrm{M}_1\,\mathbf{r}_{K_1} \quad (37)$$

wherein: ${}^f\mathbf{M}_1 = \begin{bmatrix} \cos\phi_1 & -\sin\phi_1 & 0 \\ \sin\phi_1 & \cos\phi_1 & 0 \\ 0 & 0 & 1 \end{bmatrix}$

And ϕ_1 is the rotation angle of the driving gear around O_1.

6. CASE STUDIES

In the previous sections, the mathematical model of the novel curve has been built in order to generate the NCGs tooth profile. Where: (i) Equation (6) is established for the profile of the rack cutter based on the novel curve; (ii) Equation (14) is the condition of curve convexity for the tooth profile; (iii) Equations (17), (27) and (32) expressed the mathematical model of the NCGs profiles; (iv) Equations (34), (35) and (36) provided condition for avoiding undercutting when applying the novel curve in the generation of the NCGs tooth profile; (v) Equation (37) expressed the mathematical model of the line of meshing of the NCGs pair. Based on those results, a software program has been developed to calculate, examine and design the NCGs pair. The following case studies will illustrate steps in the NCGs design process using the novel curve. The input data for the design process are provided in Tables 1 and 2.

Example 1 Design the external NCGs pair with profile generated from the rack cutter, of which the design parameters are taken from Tables 1 and 2: $\beta = 0^o$; $\lambda = 1.29$; $a = 1.75$ mm; $b = 1.36$ mm; the pitch of the rack $p_c = 19.6$ mm; the tooth height $h = 7$ mm with addendum $h_a = 3.5$ mm and dedendum $h_f = 3.5$ mm.

The gear ratio function in Figure 9 is established by the set of kinematic parameters of the NCGs pair (given in Table 3). Wherein: $R = z_1 p_c / 2\pi$, the number of teeth of the driving gear $z_1 = 8$.

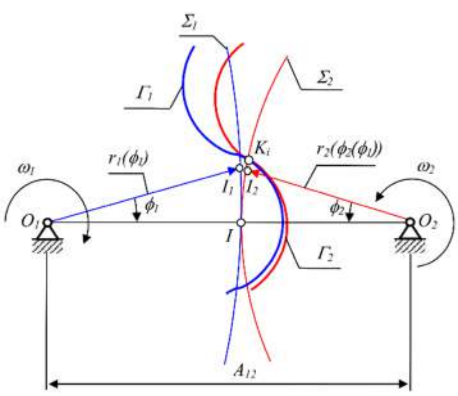

Figure 8. The line of meshing of the external NCGs pair

TABLE 3. The set of kinematic parameters of the NCGs

Parameter	Notation	Value
Center distance (mm)	A_{12}	98.86
Pitch radius Σ_1(mm)	R	25.00
Eccentric driving gear (mm)	e	5.00
Cycle coefficient	n	3.00

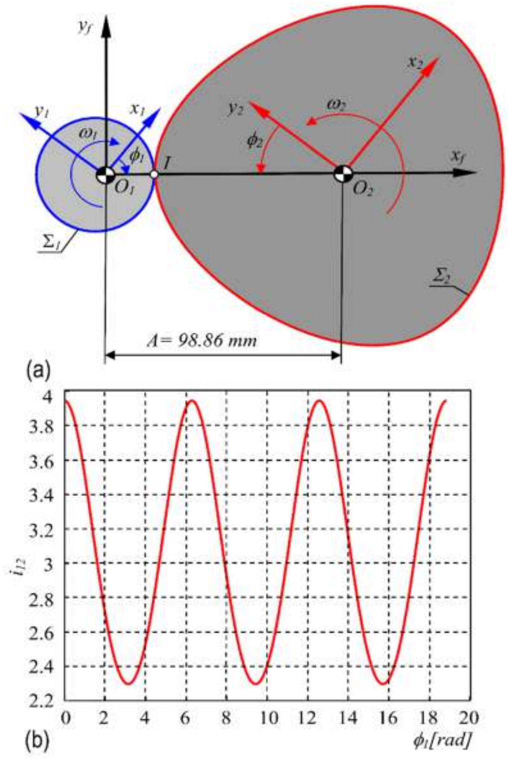

Figure 9. The NCGs pair with (a) conjugated centrodes and (b) gear ratio function

From the design parameters of the rack cutter and from the kinematic parameters of the NCGs pair, it is noticeable that for correct meshing, both of the gears need to be fabricated by the same rack cutter and $t_1 = w_1 = t = w$ can be determined by Equation (7).

It is also necessary to verify Equations (34), (35) and (36) to check condition for avoiding undercutting phenomenon (Figure 10). The design parameters of the NCG pair are calculated and presented in Table 4. Figure 11 shows the NCGs pair as well as the line of meshing.

Figure 10 shows that the novel profile avoids undercutting since there is no singularity.

From Figure 11, one obtains: (1) All of the teeth of the NCGs are identical in shape. Even in position (II) (see Figure 11a), where the curvature radius of the centrode $\rho_{II} = 48.03$ mm has a smaller value than the curvature radius in position (I) with $\rho_I = 155.52$ mm, the teeth in both positions have identical shape and equal parameters. Same as standard cylindrical gears with the constant gear ratio, so this is an advantage of the novel profile; (2) The line of meshing of the NCGs pair is a smooth closed curve (see Figure 11b), which is entirely different from the straight line when the tooth profile of the NCGs pair is involute of a circle or arcs [7, 10, 12, 22].

Example 2 This case aims to examine the influence of position of the point K_R, which lays on Σ_E, on the tooth height. Chosen from Tables 1 and 2 are those values $\lambda = 0.78$, $\beta = 90^o$, $h = 5.4$ mm, the other parameters of the rack cutter and kinematic parameters of the NCGs, as well as the design steps, are selected similarly as in Example 1

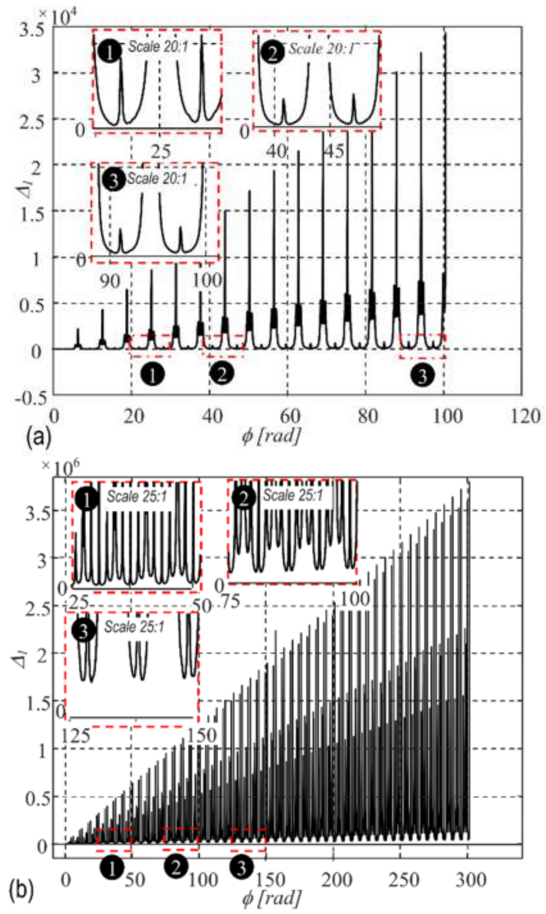

Figure 10. Condition for non-undercutting with (a) eccentric gear 1 and (b) NCGs 2

TABLE 4. Machining parameters of the NCGs pair

Parameter	Notation	Value	
		Gear1	Gear2
Center distance (mm)	A_{12}	98.9	
Number of teeth	z	8.0	24.0
Eccentric of gear1 (mm)	e	5.0	5.0
Pitch of Σ_i (mm)	p_c	19.6	19.6
Tooth thickness (mm)	t	9.8	9.8
Width of space (mm)	w	9.8	9.8
Tooth addendum (mm)	h_a	3.5	3.5
Tooth dedendum (mm)	h_f	3.5	3.5

After ensuring that the condition of non-undercutting Equations (34), (35) and (36) satisfied, the design parameters of the NCGs pair is given by Table 5. Also, Figure 12 shows the design of the gear pair.

From Figure 12 and Table 4 one obtains: (1) If the point K_R lies on the minor semi-axis of Σ_E, the generated tooth will have a shorter height, the tooth tip will be sharpened, the tooth dedendum grow larger (see Figure 12b), while the number of teeth, the pitch p_c, the tooth thickness t, and space width w remain unchanged. It also means that all the teeth still have identical shape; (2) Therefore, locating K_R on the minor semi-axis of Σ_E will increase the load capacity of the gear pair.

Example 3 This case aims to examine the influence of the position of the point K_R on the tit angle of teeth. From Table 1, λ and β can be selected as $\lambda = 1.29$, $\beta = 22.5^o$ and $\beta = 45^o$. The other parameters of the rack cutter and kinematic parameters of the NCGs are selected similarly as in the previous examples. The condition of non-undercutting Equations (34), (35) and (36) also needs to be verified. Table 5 shows the design parameters of the driven NCGs, and Figure 13 shows the final product of numerical calculation process.

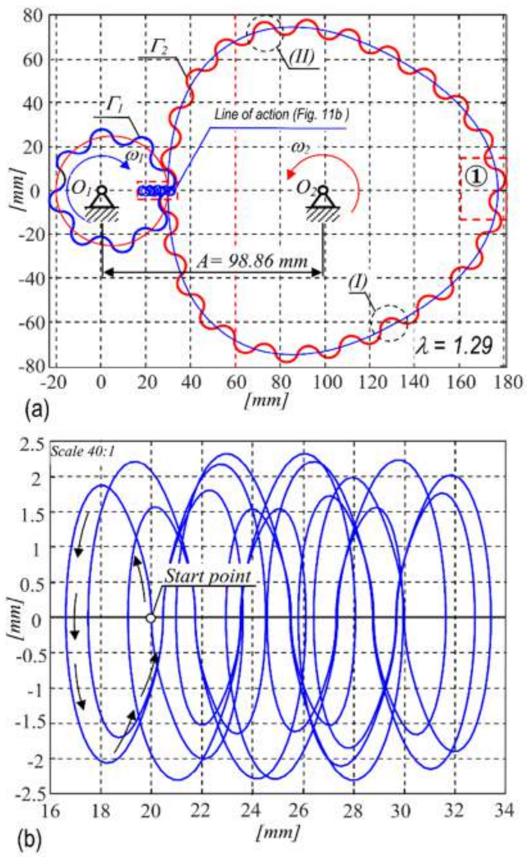

Figure 11. The external NCGs pair with $\lambda = 1.29$ (a) the tooth profile and (b) the line of meshing

From Table 5 and Figure 13 one obtains: (1) The inclination angle of the tooth decreases when β increases from 0° and the tooth height decreases. Meanwhile, the matching parameter as the pitch p_c, tooth thickness t, space width w stay unchanged; (2) Figure 13 clearly shows the tooth with steeper addendum than dedendum can help to increase the force transmission capacity from the driving to driven gear. However, this case can only be applied in the gear pair with rotation direction determined in advance and stay unchanged during working time.

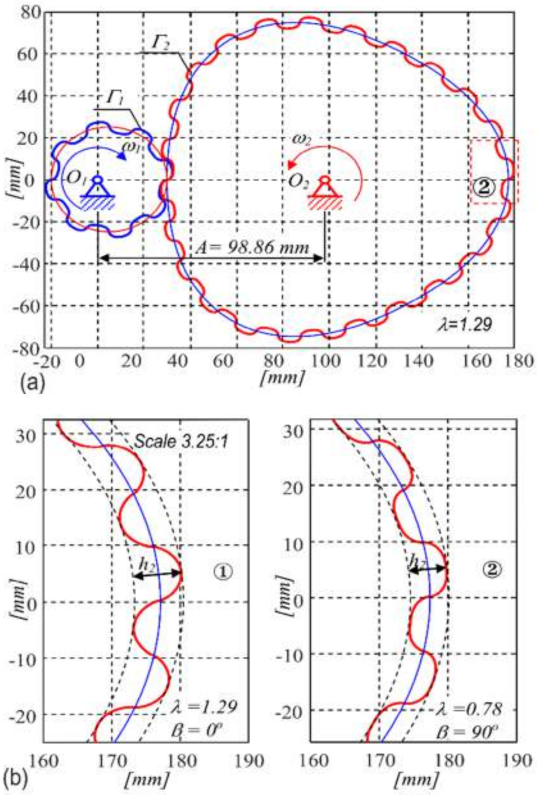

Figure 12. Examination of the generating process of NCGs profile in relationship with λ: (a) the NCGs pair and (b) comparison of profiles

TABLE 5. Design parameters of the NCGs

Parameter	Notation	Value	
		β=22.5°	β=45°
Number of teeth	z_i	24.00	24.00
Pitch of Σ_i (mm)	p_{ci}	19.60	19.60
Tooth thickness (mm)	t	9.80	9.80
Width of space (mm)	w	9.80	9.80
Tooth addendum (mm)	h_a	3.4	3.2
Tooth dedendum (mm)	h_f	3.4	3.2

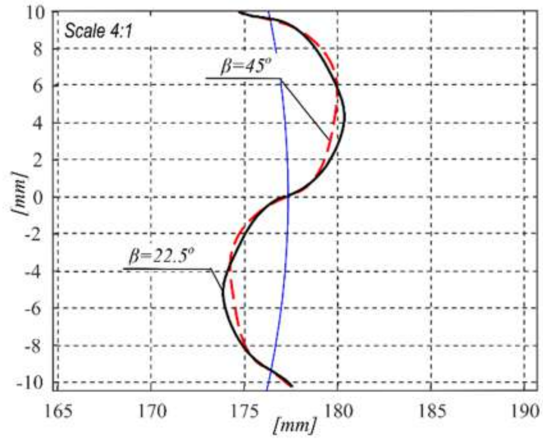

Figure 13. Profiles of the NCGs corresponding to the values of β

7. EXPERIMENTAL MANUFACTURE AND MEASUREMENT

7. 1. Experimental Manufacture of the NCGs Pair

From the above theoretical research results, a design plan with: Generating ellipse Σ_E has a semi-major axis a = 1.8 mm, a semi-minor axis b = 1.4 mm; Eccentric gear has parameters: eccentricity e = 5 mm, the centrode Σ_1 has a radius R = 25 mm, module m = 6.2 mm, Number of teeth z_1 = 8, Pitch of the centrode p_c = 19.6 mm, Tooth addendum h_a = 3.5 mm, Tooth dedendum h_f = 3.5 mm; Non-circular gears have the following parameters: Cycle coefficient n = 3, Number of teeth z_2 = 24, Pitch of the centrode p_c = 19.6 mm, Tooth addendum h_a = 3.5 mm, Tooth dedendum h_f = 3.5 mm; Center distance of gears pair A_{12} = 99 mm. Figure 14 shown below is a picture of a gears pair after manufacturing with the above design parameters.

The processing machine is the wire electric discharge machine ST3240VM (Taiwan, China) with manufacturing parameters: Wire diameter is 0.18 mm, maximum cutting speed is 200 mm/min; The electrical pulse frequency is 15.625 Hz. The dielectric is Buhm woo- BW EDM -100. The work piece gears are steel 40X.

7. 2. Experimental Measurement of Gear Ratio for the NCGs Pair

7. 2. 1. The Hardware Structure of the Experimental System The experimental system consists of an NCG pair and hardware devices, is shown in Figure 15. The rotation speed of the gear shafts 1 and 2 are determined independently by encoders with a resolution of 600 pulses. The counter of the PLC collects measurement data from the two encoders. Data from

PLC is sent to the industrial computer for processing through software. The speed from the motor shaft is transmitted to the gear shaft 1 by a belt drive with a 1:1 speed ratio to avoid overload. The computer controls motor speed through PLC to Delta inverter.

7. 2. 2. Experimental Measurement of Gear Ratio

Setting parameters: the sampling interval T = 0.1 s, motor speed 45 rpm, lubricated for NCG pair by shell grease Gadus s2 v2020-2.

After processing the data and set the standard point "**0**" of the graph, we have a comparison graph between theory and experimental measurement from the meshing process of the NCG pair as described in Figure 16.

From the measurement results, the measured values of the gear ratio for the gear pair are basically in agreement with the theoretical values. Some deviations were due to machining accuracy, assembly accuracy, measurement accuracy, and other factors. The deviations were all within the range of 0.1to 3.57% are reasonable. Thereby verified the feasibility and rationality of the new profile proposed by this study in the geometric design of NCG pairs.

Figure 14. The prototypes of the NCGs pair after manufacture

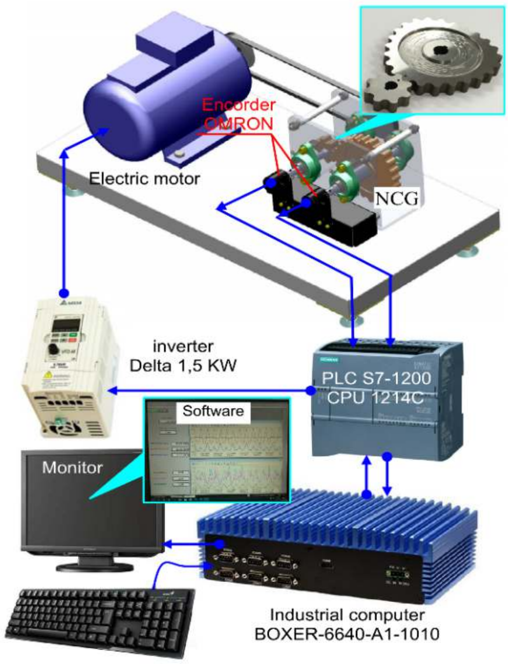

Figure 15. Experimental setup

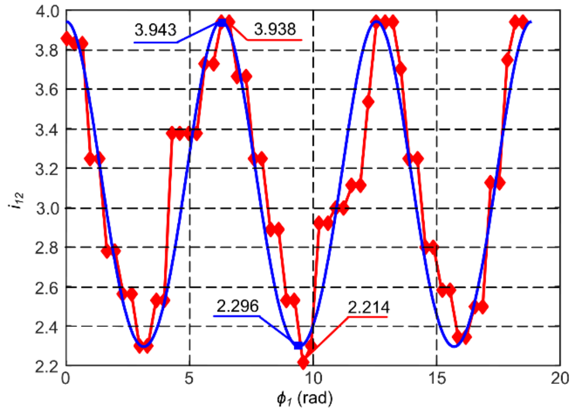

Figure 16. Gear ratio measured experimentally from the meshing of NCG pair

The above results show the difference between this study versus previous studies. Therefore, this study provides a novel profile reference in the NCG design for the theory of gearing. Also, with high load capacity, can apply the novel profile proposed by this study to design non-circular gear drives for high torque equipment such as trailing edge flap system of wind turbine rotor blade or helicopter blade [30], bowling machines [31] or steering controller of tracked vehicles [32].

8. CONCLUSIONS

This paper proposes a novel profile and provides conditions to avoid the tooth addendum concave when applied to design tooth profiles of the NGCs. Examples to illustrate the design method of the NCGs with novel profiles have been presented. Also, a gear drive was designed, manufactured and experimentally measured to verify the applicability of the novel profiles in the tooth design of the NCGs. From there, conduct evaluation and discussion to come up with some main results as follows:

i) Proposed the novel curve applied in the design of NCGs with the following advantages: (a) All the teeth at different positions of the gear are of a similar shape. Thus, this is the advantage of the proposed novel profile. It is verified via illustrative examples and experimental measurement on the manufactured NCG pair prototype and (b) Tooth thickness and width of space on the centrode of all teeth are equal.

(ii) Determined the condition of the parameters *a, b* of the generating ellipse Σ_E for avoiding concave addendum and dedendum of the gear. Therefore, it is possible to apply these conditions to write a program module that automates the design of NCGs on a computer.

(iii) With tooth profile of NCGs is the novel profile proposed by this study. The meshing line is a smooth closed curve. Unlike other profiles such as the involute of a circle or circular-arc commonly used in NCG design research, the meshing line is a straight line.

However, the limitation of this study has not mentioned the contact ratio, power transmission and gear performance. Thus, it will be considered part of our future research goals.

9. ACKNOWLEDGEMENTS

This work was supported by Project of Ministry of Education and Training, Vietnam, under grant Number: B2019 - BKA – 09.

10. REFERENCES

1. Litvin, F.L., Gonzalez-Perez, I., Fuentes, A. and Hayasaka, K., "Design and investigation of gear drives with non-circular gears applied for speed variation and generation of functions", ***Computer Methods in Applied Mechanics Engineering***, Vol. 197, No. 45-48, (2008), 3783-3802, doi: 10.1016/j.cma.2008.03.001.
2. Guo, L. and Zhang, W., "Kinematic analysis of a rice transplanting mechanism with eccentric planetary gear trains", ***Mechanism Machine Theory***, Vol. 36, No. 11-12, (2001), 1175-1188, doi: 10.1016/S0094-114X(01)00052-0.
3. Zhao, X., Chu, M., Ma, X., Dai, L., Ye, B. and Chen, J., "Research on design method of non-circular planetary gear train transplanting mechanism based on precise poses and trajectory optimization", ***Advances in Mechanical Engineering***, Vol. 10, No. 12, (2018), 1687814018814368, doi: 10.1177/1687814018814368.
4. Zhao, X., Ye, J., Chu, M., Dai, L. and Chen, J., "Automatic scallion seedling feeding mechanism with an asymmetrical high-order transmission gear train", ***Chinese Journal of Mechanical Engineering***, Vol. 33, No. 1, (2020), 1-14, doi: 10.1186/s10033-020-0432-9.
5. Ottaviano, E., Mundo, D., Danieli, G.A. and Ceccarelli, M., "Numerical and experimental analysis of non-circular gears and cam-follower systems as function generators", ***Mechanism Machine Theory***, Vol. 43, No. 8, (2008), 996-1008, doi: 10.1016/j.mechmachtheory.2007.07.004.
6. Xu, G., Hua, D., Dai, W. and Zhang, X., "Design and performance analysis of a coal bed gas drainage machine based on incomplete non-circular gears", ***Energies***, Vol. 10, No. 12, (2017), 1933, doi: 10.3390/en10121933.
7. Li, J., Wu, X. and Mao, S., "Numerical computing method of noncircular gear tooth profiles generated by shaper cutters", ***The International Journal of Advanced Manufacturing Technology***, Vol. 33, No. 11, (2007), 1098-1105, doi: 10.1007/s00170-006-0560-0.
8. Emura, T. and Arakawa, A., "A new steering mechanism using noncircular gears", ***JSME International Journal. Ser. 3, Vibration, Control Engineering, Engineering for Industry***, Vol. 35, No. 4, (1992), 604-610, doi: 10.1299/kikaic.57.154.
9. Danieli, G. and Mundo, D., "New developments in variable radius gears using constant pressure angle teeth", ***Mechanism Machine Theory***, Vol. 40, No. 2, (2005), 203-217, doi: 10.1016/j.mechmachtheory.2004.06.005.
10. Bair, B.-W., "Computerized tooth profile generation of elliptical gears manufactured by shaper cutters", ***Journal of Materials Processing Technology***, Vol. 122, No. 2-3, (2002), 139-147, doi: 10.1016/S0924-0136(01)01242-0.
11. Thai, N.H., Ly, T.T.K. and Trung, N.T., "Research design and experimental manufacturing of compound non-circular gear train with an improved cycloid profile of the ellipse", in International Conference on Engineering Research and Applications, Springer. (2021), 813-825.
12. Bair, B., "Computer aided design of non-standard elliptical gear drives", ***Proceedings of the Institution of Mechanical Engineers, Part C: Journal of Mechanical Engineering Science***, Vol. 216, No. 4, (2001), 473-482, doi: 10.1243/0954406021525250.
13. Bair, B.-W., Sung, M.-H., Wang, J.-S. and Chen, C.-F., "Tooth profile generation and analysis of oval gears with circular-arc teeth", ***Mechanism Machine Theory***, Vol. 44, No. 6, (2009), 1306-1317, doi: 10.1016/j.mechmachtheory. 2008. 07.003.
14. Litvin, F.L., Gonzalez-Perez, I., Yukishima, K., Fuentes, A. and Hayasaka, K., "Generation of planar and helical elliptical gears by application of rack-cutter, hob, and shaper", ***Computer Methods in Applied Mechanics Engineering***, Vol. 196, No. 41-44, (2007), 4321-4336, doi: 10.1016/j.cma.2007.05.003.
15. Mundo, D., "Geometric design of a planetary gear train with non-circular gears", ***Mechanism Machine Theory***, Vol. 41, No. 4, (2006), 456-472, doi: 10.1016/j.mechmachtheory.2005.06.003.
16. Zheng, F., Hua, L., Han, X., Li, B. and Chen, D., "Synthesis of indexing mechanisms with non-circular gears", ***Mechanism Machine Theory***, Vol. 105, (2016), 108-128, doi: 10.1016/j.mechmachtheory.2016.06.019.
17. Changbin, D., Yongping, L. and Yongqiao, W., "Dynamic meshing characteristics of elliptic cylinder gear based on tooth contact analysis", ***International Journal of Engineering, Transaction A: Basics***, Vol. 33, No. 4, (2020), 676-685, doi: 10.5829/ije.2020.33.04a.19.
18. Xu, H., Fu, T., Song, P., Zhou, M., Fu, C.W. and Mitra, N.J., "Computational design and optimization of non-circular gears", in Computer Graphics Forum, Wiley Online Library. Vol. 39, No. 2, (2020), 399-409.
19. García Hernández, C., Kyratsis, P., Gella-Marín, R., Efkolidis, N. and Huertas-Talón, J., *Wedm manufacturing method for noncircular gears, using cad/cam software*. 2016.
20. Liu, Y., Han, J., Xia, L. and Tian, X., "Hobbing strategy and performance analyses of linkage models for non-circular helical gears based on four-axis linkage", ***Strojniški vestnik-Journal of Mechanical Engineering***, Vol. 58, No. 12, (2012), 701-708, doi: 10.5545/sv-jme.2012.524.
21. Liu, Y. and Diao, J., "Six-axis linkage strategy and its models for non-circular helical gears based on diagonal hobbing/strategija in modeli sestosnega diagonalnega odvalnega rezkanja neokroglih zobnikov s posevnim ozobjem", ***Strojniški Vestnik-Journal of Mechanical Engineering***, Vol. 61, No. 5, (2015), 330-342, doi: 10.5545/sv-jme.2014.2371.
22. Thai, N.H., Thom, P.V. and Trung, N.T., "Influence of centrodes coefficient on the characteristic of gear ratio function of the compound non-circular gear train with improved cycloid tooth profile", in IFToMM Asian conference on Mechanism and Machine Science, Springer. (2021), 204-214.

23. Zheng, F., Hua, L., Han, X., Li, B. and Chen, D., "Linkage model and manufacturing process of shaping non-circular gears", ***Mechanism Machine Theory***, Vol. 96, (2016), 192-212, doi: 10.1016/j.mechmachtheory.2015.09.010.
24. Chen, C.-F. and Tsay, C.-B., "Computerized tooth profile generation and analysis of characteristics of elliptical gears with circular-arc teeth", ***Journal of Materials Processing Technology***, Vol. 148, No. 2, (2004), 226-234, doi: 10.1016/j.jmatprotec.2003.07.011.
25. Changbin, D., Yongping, L. and Yongqiao, W., "Meshing error of elliptic cylinder gear based on tooth contact analysis", ***International Journal of Engineering, Transaction A: Basics***, Vol. 33, No. 7, (2020), 1364-1374, doi: 10.5829/ije.2020.33.07a.24.
26. Khodadadi, M., Khalili, K. and Ashrafi, A., "Studying the effective parameters on teeth height in internal gear flowforming process", ***International Journal of Engineering, Transaction C: Aspects***, Vol. 33, No. 12, (2020), 2563-2571, doi: 10.5829/ije.2020.33.12c.18.
27. Bigdeli, M. and Monfared, V., "The prediction of stress and strain behaviors in composite gears using fem", ***International Journal of Engineering, Transaction B: Applications***, Vol. 34, No. 2, (2021), 556-563, doi: 10.5829/ije.2021.34.02b.29.
28. Litvin, F.L., Gonzalez-Perez, I. and Fuentes-Aznar, A., "Noncircular gears, Cambridge University Press, (2009).
29. Litvin, F.L. and Fuentes, A., "Gear geometry and applied theory, Cambridge university press, (2004).
30. Ha, K., "Innovative blade trailing edge flap design concept using flexible torsion bar and worm drive", ***HighTech Innovation Journal***, Vol. 1, No. 3, (2020), 101-106, doi: 10.28991/HIJ-2020-01-03-01.
31. Furch, J. and Nguyen, Q.H., "Lifetime test of tracked vehicle torsion bars using monte carlo method", ***Emerging Science Journal***, Vol. 4, No. 5, (2020), 376-389, doi.
32. Bickramdass, R., Persad, P. and Loutan Jr, K., "Evaluation of an anthropometric fast bowling machine", ***HighTech Innovation Journal***, Vol. 2, No. 2, (2021), 108-119, doi: 10.28991/HIJ-2021-02-02-04.

Persian Abstract

چکیده

این مقاله یک منحنی جدید را ارائه می‌کند که توسط یک نقطه متصل به یک بیضی در حالی که بدون لغزش در امتداد خط مبدأ قفسه برش می‌چرخد، ایجاد می‌شود. یک مدل ریاضی از مشخصات دنده غیر دایره ای بر اساس تئوری چرخ دنده توسعه داده شده است. اثر یک نسبت محوری λ (نسبت طول محورهای اصلی و فرعی بیضی) و موقعیت نقطه KR که در آن منحنی جدید شروع به ایجاد می‌کند بر روی شکل دندان و زیر بریدگی دندان غیر جفت دنده دایره ای نیز در نظر گرفته شده است. یک برنامه عددی توسعه یافته از مدل ریاضی برای محاسبه و طراحی چرخ دنده های غیر دایره ای (NCGs)پیشنهاد شده است. مطالعات موردی برای نشان دادن مراحل طراحی شکل دندان و بررسی مشخصات هندسی NCGs در رابطه با پارامترهای طراحی رک کاتر و غیره ارائه شد. را می توان برای هر مورد خاص به منظور طراحی پروفایل های مناسب NCG ها انتخاب کرد. بر این اساس، آزمایشی برای تعیین نسبت دنده جفت NCGs بر اساس مش بندی بین چرخ دنده ها ساخته شده است.